ACS APPLIED MATERIALS & INTERFACES

Research Article

www.acsami.org

Printing Small Dots from Large Drops

Emma L. Talbot,[†] Huai N. Yow,[§,¶] Lisong Yang,[†] Arganthaël Berson,[‡,⊥] Simon R. Biggs,[§,∥] and Colin D. Bain*[,†]

[†]Department of Chemistry and [‡]School of Engineering and Computing Sciences, Durham University, South Road, Durham, DH1 3LE, U. K.

[§]Institute of Particle Science and Engineering (IPSE), School of Process, Environmental and Materials Engineering, University of Leeds, Leeds LS2 9JT, U. K.

Supporting Information

ABSTRACT: Printing of droplets of pure solvents containing suspended solids typically leads to a ring stain due to convective transport of the particles toward the contact line during evaporation of the solvent. In mixtures of volatile solvents, recirculating cells driven by surface tension gradients are established that lead to migration of colloidal particles toward the center of the droplet. In favorable cases, a dense disk of particles forms with a diameter much smaller than that of the droplet. In the latter stages of drying, convective transport of the particles radially toward the contact line still occurs. Two strategies are described to fix the distribution of particles in a compact disk much smaller than the initial diameter of the drying droplet. First, a nanoparticulate clay is added to induce an evaporation-driven sol−gel transition that inhibits convective flow during the latter stages of drying. Second, a nonadsorbing polymer is added to induce depletion flocculation that restricts particle motion after the particles have been concentrated near the center of the droplet. The area of the resulting deposit can be as little as 10% of the footprint of the printed droplet.

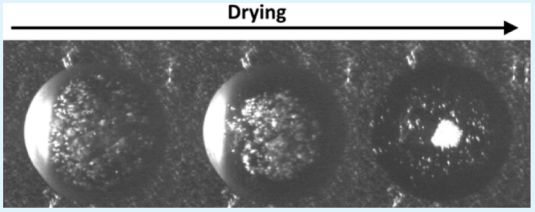

KEYWORDS: *droplet deposition, ink-jet printing, drying, sol−gel transition, depletion flocculation*

INTRODUCTION

Ring stains are the common result of the evaporation of droplets containing dissolved solutes or suspended solids. The coffee ring left by spilt coffee is one familiar example. A ring stain arises in pinned droplets due to evaporation of the solvent near the edge of the droplet. To maintain the spherical cap shape of the droplet, capillary flow replenishes solvent lost due to evaporation, transporting particles to the contact line.[1,2] In ink-jet-printing applications, the resulting dot has lower optical density at the center compared to the edge, leading to poor image quality and the need for an excess of ink to generate a desired depth of color. Nonuniform deposits are also detrimental to ink-jet-printing applications such as organic electronics,[3−6] printed circuit-boards,[7−10] and biomedicine (e.g., microassays).[11,12] Internal flows driven by surface-tension gradients—known as Marangoni flows—have been used to counteract the formation of a ring stain and produce more uniform deposits,[13−17] enhancing print quality or performance.

Marangoni flows can be induced by thermal gradients, by surfactants, or by differential evaporation in solvent mixtures (a well-known example being the tears of wine in a glass).[13,18,19]

The evaporation-driven Marangoni flows in ethanol/water mixtures not only recirculate particles within the droplet but also lead to migration of particles across the streamlines toward the center of the droplet[20,21] (see Figure 1). Particle migration creates a concentrated central group of particles and a region near the contact line that is depleted of particles. At some stage during the evaporation, the Marangoni recirculation abruptly ceases (Figure 1iii) and is replaced by evaporation-driven radial flow that transports particles toward the contact line, leading to dissipation of the collected group (Figure 1iv,v). The final result is a ring stain (Figure 1vi).[21] The migration is not limited to ethanol/water mixtures but is only observed within picoliter droplets.

The driving force for the cross-stream migration is still not entirely clear, and various possible mechanisms will be considered in a separate paper. Here, we concern ourselves with the practical question of how we can "fix" the particle distribution in a concentrated central disk before radial flow transports particles to the periphery. The concept of printing a dot with a diameter much smaller than the initial droplet footprint could be extended to lines of coalesced droplets, which would allow the printing of wires or tracks much finer than the droplets used to print the lines. In this paper, we describe and compare two strategies. The first strategy involves addition of a nanoparticulate clay. As the droplet evaporates, the concentration of the clay increases to the point where it undergoes a sol−gel transition. The resulting elasticity in the droplet dominates the capillary forces and inhibits the formation of a ring stain.[22] We have shown previously that the sol−gel transition in pure water droplets can be used to generate a deposit with a uniform profile. The challenge here is to time

Received: December 10, 2014
Accepted: January 23, 2015
Published: January 23, 2015

DOI: 10.1021/am5087177
ACS Appl. Mater. Interfaces 2015, 7, 3782−3790

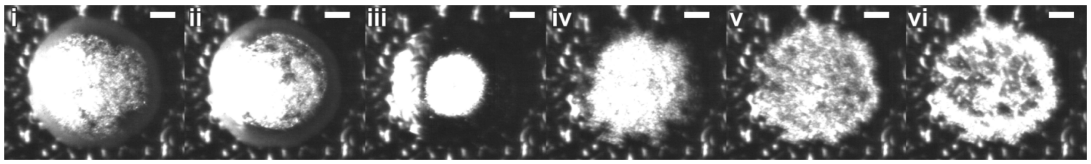

Figure 1. Dark-field images of a drying 50 vol % ethanol/water droplet containing 0.1 vol % of 1 μm polystyrene spheres after (i) $0.1t_{dry}$, (ii) $0.2t_{dry}$, (iii) $0.5t_{dry}$, (iv) $0.8t_{dry}$, (v) $0.9t_{dry}$, and (vi) $1.0t_{dry}$ (where t_{dry} = 2.80 s). Scale bars are 20 μm.

gelation to coincide with the minimum in the diameter of the collected group of particles. The second strategy involves the addition of a nonadsorbing polymer that is excluded from the region between colloidal particles and induces an attractive, osmotic force between them. As the droplet evaporates, the polymer concentration, and hence the attractive force, increases, leading to aggregation of the particles, a process known as depletion flocculation. The challenge is to induce flocculation of the collected particles into a single, connected aggregate without premature aggregation that leads to a lumpy deposit. The physical chemistry of these two strategies is described in greater detail below.

Sol−Gel Transition. Laponite (a nanoparticulate clay) forms shear-thinning suspensions that can be jetted from an ink-jet printhead. The high shear in the printhead breaks down the networked structure of the laponite suspension. As the droplet dries, the laponite is concentrated and the network recovers, undergoing a sol−gel transition.[22] The increased yield stress and elastic modulus of the gel[23] can allow deformation of the droplet geometry from a spherical cap, resisting the capillary flow that otherwise results in radial particle motion. We define a dimensionless number

$$\varepsilon = G' r_c / 2\sigma \quad (1)$$

as the ratio of the elastic modulus (G') to the Laplace pressure ($p = 2\sigma/r_c$) inside the droplet, where r_c is the radius of curvature of the droplet and σ is the surface tension. In order to resist deformation, ε must be at least 1. For a 50 vol % ethanol/water suspension with surface tension σ = 29 mN m^{-1}, droplet height h = 7 μm, contact radius R = 80 μm, and contact angle θ = 10°, the Laplace pressure p = 126 Pa [where the radius of curvature $r_c = (R^2+h^2)/2h$]. Therefore, G' must be on the order of 10^2 Pa to prevent particle motion toward the contact line. Note that p depends on the radius of curvature. If the droplet dries with a constant contact angle (receding contact line), p increases during drying. In the presence of suspended solids, it is much more common for the contact line to be pinned and then p decreases during drying.

For droplets with a contact angle below 90° evaporating in an open air environment, evaporation is fastest at the contact line.[1] The droplet is also thinner near the contact line, and hence, the laponite concentration increases fastest near the periphery of the droplet: it is here that the suspension gels first. A gelling front propagates from the contact line inward, preventing particle motion in the gel. Figure 2 illustrates this process for polystyrene spheres in a pure water droplet. (In pure water, there is no cross-stream migration and so there are particles throughout the droplet to enable us to visualize the flow.) Varying the initial laponite concentration enables us to induce gelation at the time when the particles are most densely packed near the droplet center and thus to prevent radial flow outward at the end of drying.

Depletion Flocculation. The alternative fixing strategy explored in this paper uses a nonadsorbing polymer (polystyrenesulfonate) to induce depletion flocculation of the particles once they have migrated to the center of the droplet. Depletion flocculation[24−26] can occur when particles approach each other to less than twice the radius of gyration of the polymer. It is energetically more favorable for the polymer to leave the gap between the particles than to change its conformation in order to fit within the restricted volume between approaching particles. As a consequence, the water solvent between the particles has a lower polymer concentration than the bulk solution and there is an osmotic pressure forcing the particles together. The strength of the depletion force and the compactness of the aggregates depend on the concentration and molecular weight of the polymer and on the particle concentration.[27] Lower molecular weight polymers lead to a shallower minimum in the free energy, since the particles need to be closer together before the polymers are excluded from the contact (and hence the osmotic pressure acts over a shorter range). The weaker depletion interaction allows reversible detachment and rearrangement of particles, resulting in a denser and more compact floc. However, a higher polymer concentration is required to induce flocculation at lower polymer molecular weights. Since aggregation involves the loss of translational entropy of particles, higher polymer concentrations are also required to aggregate particles at lower particle concentrations. During evaporation, both the polymer concentration and the particle density increase, favoring flocculation.

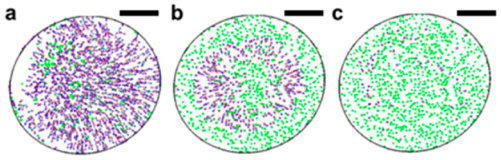

Figure 2. Particle tracks within a drying droplet of 2 wt % laponite in pure water between (a) $0.0t_{dry}$ and $0.1t_{dry}$, (b) $0.4t_{dry}$ and $0.5t_{dry}$, and (c) $0.7t_{dry}$ and $0.8t_{dry}$ (where t_{dry} = 6.32 s). Stationary particles are in green, and moving particles are in blue with their initial position marked in red. The contact line is marked by a black ellipse. Scale bars are 50 μm.

EXPERIMENTAL METHODS

Ink-jet droplets were formed with a Microfab device (MJ-ABP-01, Plano, Texas; 50 μm diameter orifice) controlled by a Microfab JetDrive III controller. The waveform used for printing was adjusted to ensure the ejection of single droplets with no satellites. The particle distribution inside a drying droplet was imaged on an inverted microscope using dark-field illumination.[21] Images were acquired at 250 frames per second with an exposure of 100 μs (Photron APX RS) through the substrate. Transparent glass substrates were plasma-coated with a hydrophobic layer as described in ref 28 to increase contact angles. The drying time, t_{dry}, was defined as the time when the refractive index contrast of the beads changed due to loss of the solvent surrounding the beads.

Sol−Gel Mechanism. Laponite suspensions (RD grade, Rockwood; disks 30 nm across and 1 nm thick, according to the manufacturer's specifications) were prepared in ethanol/water mixtures. The laponite was first added gradually, with agitation, to high-purity water (Milli-Q) or to a suspension of polystyrene spheres (1 μm diameter, 0.1 vol % concentration, University of Leeds; preparation in ref 29) and sonicated

DOI: 10.1021/am5087177
ACS Appl. Mater. Interfaces 2015, 7, 3782−3790

until the laponite formed a clear suspension. Ethanol (Sigma-Aldrich, 99.9%) was then added and the mixture was sonicated until clear. The order of addition was important, as adding the laponite to an ethanol/water mixture resulted in a cloudy flocculated suspension, even after sonication. The laponite does not alter the surface tension enough to prevent solutal Marangoni flows.[30]

Depletion Flocculation. Polystyrenesulfonate (PSS) was used as the nonadsorbing polymer with the following molecular weights: 35 kg mol^{-1} (Scientific Polymer Products Inc.), 70 kg mol^{-1} (Sigma-Aldrich), 300 kg mol^{-1} (Alfa Aesar), and 500 kg mol^{-1} (Alfar Aesar). The PSS was dissolved in high-purity water and left overnight. Ethanol was then added and the solution was shaken to ensure homogeneous mixing. Lastly, 755 nm polystyrene spheres (University of Leeds, in ethanol) were added to give a concentration of 0.1 vol %.

Rheological data for laponite suspensions were collected at 293 K in an AR 2000 rheometer (TA Instruments) with a cone (2° angle) and plate geometry, without the inclusion of polystyrene spheres. The steady-state viscosity of each fluid was recorded over shear rates from 0.001 to 1500 s^{-1}. Recovery times were investigated by applying a stepped shear rate with fast sampling. The shear rate was held at 0.1 s^{-1} for 10 min and then 1000 s^{-1} for 4 min, before returning to the low shear value (0.1 s^{-1}). The yield stress of each laponite suspension was found using oscillatory measurements with small deformations, performed with a strain sweep (for strain values between the rheometer's lower limit of 2.88×10^{-3} and 0.35) at a frequency of 1 Hz. The yield stress was estimated from the product of the critical strain and the elastic modulus in the linear elastic region. The critical strain was defined as the strain at which a straight-line fit to the linear elastic region and nonlinear viscoelastic region intersected.

A LUMiSizer 611 (L.U.M. GmbH) was used to investigate the stability of polystyrene particles in suspension via centrifugal sedimentation (as in ref 29). Suspensions containing 5 vol % polystyrene spheres (630 nm, University of Leeds) were observed at varying PSS content. Samples of 400 μL were placed in a polycarbonate cell (optical path length 2.0 mm) and spun at 1500 rpm for 10 h to form an initial packed sediment bed. The centrifugation field was then increased stepwise by 500 rpm every 84 min up to a maximum of 4000 rpm. Stable particles (no aggregates) form a flat, packed bed. Aggregates are able to withstand the applied centrifugal force, forming a less compressed sediment bed, and thus giving a raised bed height (see Figure 3). Increasing the centrifugation field can further compact the bed, with weaker aggregates collapsing at lower spinning rates.

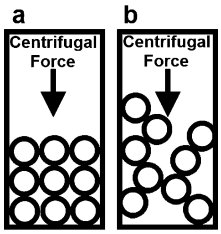

Figure 3. Schematic illustration of the sediment bed from (a) stable particles and (b) aggregated particles. The sediment bed is more compressed with a lower bed height for stable particles.

Dried deposits were imaged with a scanning electron microscope (SEM, Philips XL30 Environmental SEM) to determine the packing and distribution of the polystyrene spheres. The deposits were sputter-coated with gold (three coats at 1.2 kV, 35 mA for 30 s, Edwards Scancoat Six) before imaging.

RESULTS AND DISCUSSION

In ethanol/water mixtures, circulating flows developed during drying, coupled with particle migration. Figure 4 shows the progress of the evaporation of droplets of ethanol/water mixtures of varying compositions, imaged through the substrate. The radius of the particle group, R_g (see Figure 5), decreased throughout the Marangoni flow period, reaching a minimum radius, $R_{g,min}$, at a time, t_{R_g}, that coincided with the point when Marangoni flow ceased. Subsequently, capillary flow transported particles toward the contact line, increasing R_g again (see Figure 1; not shown in Figure 4).

Particle migration was most pronounced in lower ethanol concentrations (10−50 vol %) with $R_{g,min}$ reaching a minimum value of 0.34 for 30 vol % ethanol. At 70 vol % ethanol, the collected group was twice as wide, and for 90 vol % ethanol no particle migration was evident. Therefore, water-rich mixtures produce the most concentrated particle groups.

Sol−Gel Fixing Strategy. Control of the rheology of the laponite/ethanol/water suspension is essential to fix the distribution of polystyrene particles at the minimum radius, R_g. If the suspension gels too late, the particles will be transported outward by capillary flow. If the viscoelasticity increases too soon, the Marangoni flows and particle migration will be suppressed. At the same time, the high-shear rheology must be compatible with ink-jet printing. Figure 4 shows that particle migration is most pronounced in mixtures that are initially ≤50 vol % ethanol. During evaporation, the concentration of ethanol drops further, so at the point of gelation the volume percent of ethanol is less than that in the original formulation. We therefore need to explore only the rheology of water-rich suspensions. We take 10 and 50 vol % ethanol as the limits of the relevant formulation space (the rheology of laponite in pure water has been described in ref 27).

Inverted bottle experiments for laponite/ethanol/water mixtures place the sol−gel transition between 2.8 and 3.0 wt % laponite in 10 vol % ethanol/water (the same as in pure water[22]) and between 1.5 and 2.0 wt % laponite in 50 vol % ethanol/water. Hence, the gel point is lowered at higher ethanol concentrations. This trend hinders the fixing strategy: as ethanol is depleted during drying, the laponite concentration required to reach the gel point increases progressively.

The shear-thinning properties of the laponite suspensions are displayed in Figure 6. The network structure responsible for the high viscosity at low shear breaks down under the shear rates in the nozzle of the printhead ($\sim 10^4$ s^{-1} for the Microfab) to give a low-viscosity fluid (viscosity, $\eta \sim 10^{-2}$ Pa s). In the 10 vol % ethanol suspension, the viscosity increased with increasing laponite concentration. For the same laponite concentration (2.5 wt %), the mixture with more ethanol had a higher low-shear viscosity but a similar high-shear viscosity. Thus, the jettability is unaffected by either the ethanol or laponite concentration within the range studied.

Table 1 displays the yield stress of the laponite suspensions shown in Figure 6. At the higher ethanol concentration, a yield stress is first observed at a lower laponite concentration (1.5 wt % laponite in 50 vol % ethanol compared to 3 wt % laponite in 10 vol % ethanol). The yield stress increased markedly with laponite concentration at 10 vol % ethanol but less so at 50 vol % ethanol. The typical Laplace pressure in a drying droplet is ∼100 Pa, so the yield stress must be at least of this order for gelation to inhibit radial capillary flows. The data in Table 1 suggest that the gel in 50 vol % ethanol may be too weak, but the gel becomes stronger as the ethanol evaporates.

It is not only the yield stress that is important for the success of our strategy but also the speed with which the laponite network recovers after a period of high shear: the minimum group radius is attained after a time $t_{R_g} \sim 1$ s for 50 pL drops. The laponite network thus needs to gel on this time scale. Figure 7 presents the

DOI: 10.1021/am5087177
ACS Appl. Mater. Interfaces 2015, 7, 3782−3790

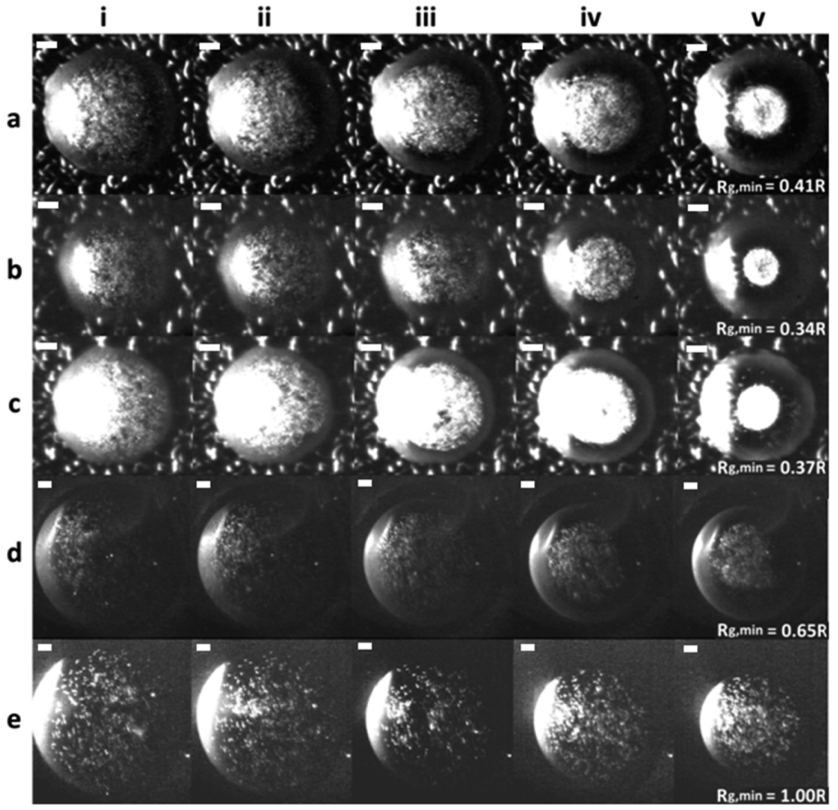

Figure 4. Drying droplets containing (a) 10 vol %, (b) 30 vol %, (c) 50 vol %, (d) 70 vol %, or (e) 90 vol % ethanol/water and 0.1 vol % of 1 μm polystyrene spheres on coated substrates after (i) $0.1t_{R_g}$, (ii) $0.2t_{R_g}$, (iii) $0.5t_{R_g}$, (iv) $0.8t_{R_g}$, and (v) $1.0t_{R_g}$. The minimum radius of the group, $R_{g,min}$, is shown as a fraction of the contact radius at time t_{R_g}. The substrates in parts d and e are the same as for parts a–c, though the illumination differs, resulting in lower contrast. The contact line retracts in parts d and e due to the higher ethanol content. Scale bars are 20 μm.

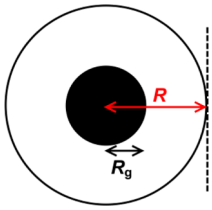

Figure 5. Schematic of the particle group (with radius R_g) in a droplet of contact radius R.

Table 1. Yield Stresses for Laponite Suspensions in Ethanol/Water Mixtures

laponite/wt %	ethanol/vol %	yield stress/Pa
2.5	10	
3.0	10	6
4.0	10	29
5.0	10	99
1.5	50	5
2.0	50	26
2.5	50	24

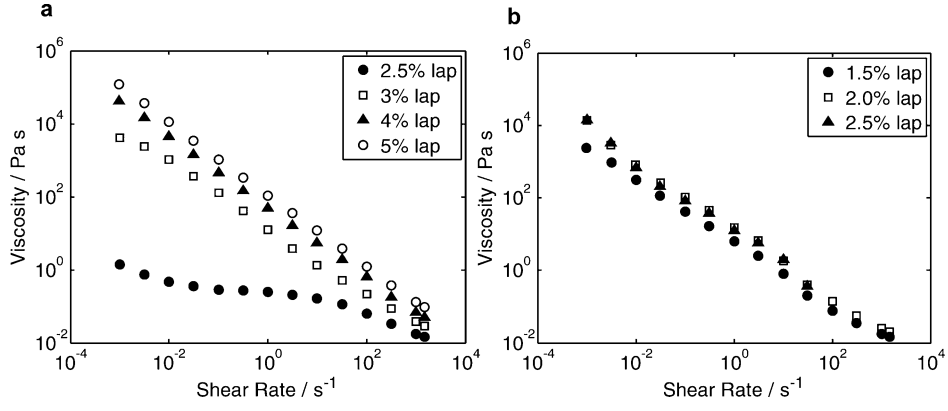

Figure 6. Shear viscosity of laponite suspensions in (a) 10 vol % ethanol/water and (b) 50 vol % ethanol, with various laponite concentrations over a range of shear rates.

DOI: 10.1021/am5087177
ACS Appl. Mater. Interfaces 2015, 7, 3782–3790

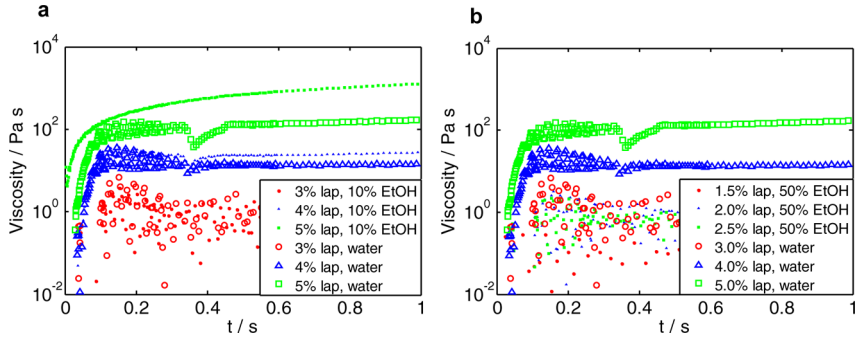

Figure 7. Recovery of the shear viscosity for laponite suspensions in (a) 10 vol % ethanol and (b) 50 vol % ethanol, compared to laponite/water suspensions with a laponite concentration following evaporation of the ethanol. The dip just before 0.4 s is an artifact due to the rheometer's response time.

recovery of the shear viscosity of laponite suspensions following a period of high shear (and then a return to a low shear rate). Although we did not measure the elasticity directly, we assume that the elasticity recovers at a comparable rate to the viscosity. For a fixed ethanol concentration, the shear viscosity recovered faster with higher laponite content. Similarly, a higher concentration of ethanol increased the speed at which the laponite network re-formed for the same laponite concentration.

As a droplet of laponite/ethanol/water dries, ethanol evaporates preferentially. Therefore, during drying, the ethanol concentration decreases and the laponite concentration increases, changing the composition toward a laponite suspension in pure water. A decrease in the ethanol content leads to an increase in the recovery time, but an increase in the laponite concentration leads to faster recovery. The combined effect is a shorter recovery time, suitable for our purpose. Figure 7 shows that the laponite network can recover within the drying lifetime for both water and ethanol/water mixtures. Note that the Marangoni flows within the droplet shear thin the laponite suspension, preventing the viscosity from ceasing the circulation, but this also requires quicker recovery once Marangoni flows cease to implement the fixing strategy. A rough estimate of the maximum shear rate due to Marangoni flows inside a droplet can be obtained from the droplet height, h, and the maximum mean flow velocity near to the substrate, u. Typically for a droplet of 50 vol % ethanol/water, the maximum flow velocity near the substrate is ~2 mm s^{-1}. Flow velocities near the liquid vapor interface are larger (~3u). For an initial droplet height of 7 μm, an estimate of the maximum shear rate is $\dot{\gamma} \sim u/h \sim 850\ s^{-1}$.

We recorded the drying behavior of 10 and 50 vol % ethanol/water mixtures with varying concentrations of laponite. For 10 vol % ethanol, laponite concentrations below 2 wt % did not gel sufficiently quickly: the particles migrated inward to form a central disk with a size similar to that in the absence of laponite but were then transported toward the contact line by radial convection in the latter part of drying. For concentrations of laponite ≥2.0 wt %, the droplet gelled from the contact line inward and halted the radial convection of the particles, fixing the centrally collected group. The minimum value of R_g in the dry deposit was obtained with 2.5 wt % laponite (Figure 8a). There was some outward motion of the collected group before the sol−gel transition suppressed convection, giving a deposit diameter of 0.6R (where R is the initial radius of the contact line), compared to a value of $R_{g,min}$ = 0.41R observed in the absence of laponite (Figure 4a). At an initial laponite concentration ≥2.8 wt %, the viscosity near the contact line rose too quickly and prevented migration of particles near the contact line toward the central

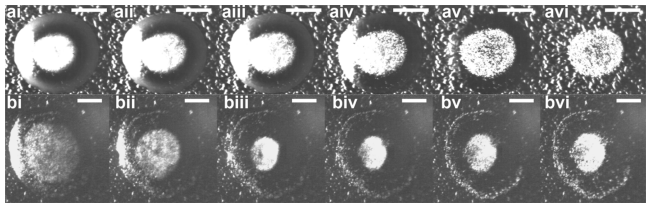

Figure 8. Images of drying droplets of laponite/ethanol/water suspensions containing 0.1 vol % of 1 μm polystyrene spheres and (a) 10 vol % ethanol with 2.5 wt % laponite and (b) 50 vol % ethanol with 1.5 wt % laponite. Images were taken after (i) 0.1t_{dry}, (ii) 0.2t_{dry}, (iii) 0.3t_{dry}, (iv) 0.5t_{dry}, (v) 0.8t_{dry}, and (vi) 1.0t_{dry}. Scale bars are 50 μm.

disk. The final deposit comprised a central dot and a ring near the contact line.

Increasing the ethanol concentration to 50 vol % ethanol gave results similar to those of 10 vol % ethanol but at lower concentrations of laponite. Figure 8b shows the smallest central dot in the dry deposit, which was obtained with 1.5 wt % laponite, but also shows the peripheral ring.

The experiments described above show that the strategy of using the sol−gel transition in laponite suspensions to fix the central disk of particles does work but that the minimum radius of the dry deposit is significantly larger than the minimum radius of the collected group in the absence of laponite. Further increases in laponite concentration led to a peripheral ring in addition to a central dot. The best results were obtained for a 10 vol % ethanol/water mixture containing 2.5 wt % laponite. We explored whether small dots could also be printed with a higher loading of particles (1 vol % polystyrene spheres). Particle migration still occurred and the sol−gel transition inhibited radial convective flow, leading to a printed dot smaller than the droplet footprint, as at the lower particle concentration (Figure 9). The radius of the particle group is wider at the higher particle loading, possibly due to collision-induced migration toward the contact line.

Depletion Flocculation. The second control strategy was based on depletion flocculation. A free polymer (polystyrenesulfonate, PSS) was included in the ethanol/water mixture. Sedimentation studies were carried out to determine the PSS concentration required to induce aggregation of the polystyrene spheres in water for PSS molecular weights of 70, 300, and 500 kg mol^{-1}. The stability against aggregation in ethanol/water was assessed to ensure that most of the ethanol would need to evaporate before there was significant aggregation of the polystyrene spheres. Otherwise, premature aggregation might

DOI: 10.1021/am5087177
ACS Appl. Mater. Interfaces 2015, 7, 3782−3790

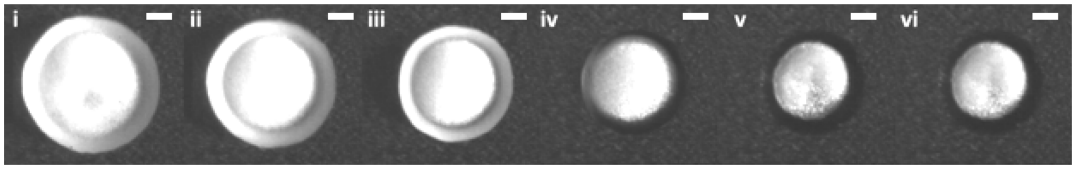

Figure 9. Sequence of images for a drying ethanol/water mixture containing 10 vol % ethanol, 2.5 wt % laponite, and 1 vol % of 775 nm polystyrene spheres on a coated glass substrate at (i) $0.1t_{dry}$, (ii) $0.2t_{dry}$, (iii) $0.5t_{dry}$, (iv) $0.8t_{dry}$, (v) $0.9t_{dry}$, and (vi) $1.0t_{dry}$. The contact line retracts on this substrate. Scale bars are 20 μm.

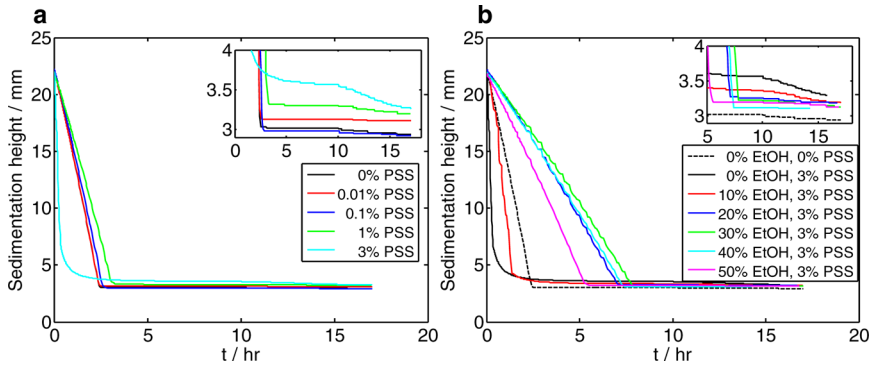

Figure 10. Sedimentation profiles of 5 vol % polystyrene spheres in (a) water with increasing PSS (70 kg mol^{-1}) concentration and (b) water with 0 wt % PSS (70 kg mol^{-1}) or ethanol/water solutions with 3 wt % PSS (in the water alone). Insets show closeups for the beds following initial compression. The centrifuge speed was held at 1500 rpm for 10 h and then increased stepwise by 500 rpm every 84 min until a maximum of 4000 rpm.

occur while the particles are migrating toward the center of the droplet.

Figure 10a shows the sedimentation profiles for 70 kg mol^{-1} PSS solutions in water at increasing PSS concentrations. At concentrations up to 0.1 wt % PSS, the similarity in the sedimentation profile to that of 0 wt % PSS indicates minimal particle aggregation. At a PSS concentration of 1 wt %, there are competing effects between the increase in viscosity due to the presence of the free polymer and the increase in the size of the floc due to particle aggregation. Sediment bed compression indicates the presence of aggregated particles (leading to a more open bed), compared to stable particles with no added PSS. At 3 wt % PSS, there is clear evidence of particle aggregation in the steeper initial sedimentation profile and stepwise bed compression profile (following the increase of the centrifuge speed after 10 h).

To formulate a PSS suspension in ethanol/water that will be stable in the printhead but induce particle flocculation as the suspension becomes water-rich during drying, the sedimentation profiles of particles within PSS (70 kg mol^{-1}) suspensions in a range of ethanol/water mixtures were investigated (see Figure 10b). Each suspension contained 3 wt % PSS in the water phase alone before dilution with ethanol to ensure flocculation on depletion of the ethanol. (From here on, PSS concentrations are given in the water alone unless stated otherwise; e.g., 3 wt % PSS corresponds to a 1.7 wt % PSS concentration in the entirety of 50 vol % ethanol/water). Figure 10b shows that ethanol/water suspensions containing 3 wt % PSS are stable if the ethanol concentration is $\geq$20 vol %. At lower concentrations of ethanol, the sediment bed was raised compared to that of 0 wt % PSS, and the steeper initial sediment profile indicates particle aggregation. Hence, an initial ethanol concentration of at least 20 vol % is required to ensure particle stability in the printhead.

Lower PSS concentrations were required to induce particle flocculation at higher molecular weights (Table 2). For each molecular weight of PSS, at least 20−30 vol % ethanol was

Table 2. PSS Concentration Required To Induce Particle Aggregation for Three Molecular Weights (MW) of the Polymer and the Minimum Ethanol Content for a Stable Suspension

MW/kg mol^{-1}	PSS for aggregation in water/ wt %	min ethanol/vol %
70	3.0	20
300	0.5	30
500	0.1	20

required for the suspension of PS particles to be stable. We chose to print particle suspensions in a 50 vol % ethanol/water mixture to ensure that the formulation was stable and did not flocculate during the migration period.

Figure 11 shows the effect on the deposit of adding 70 kg mol^{-1} PSS to a PS particle suspension in 50 vol % ethanol/water. At PSS concentrations $\leq$0.1 wt % (i.e., $\leq$0.06 wt % total in the entire suspension), drying progressed similarly to droplets

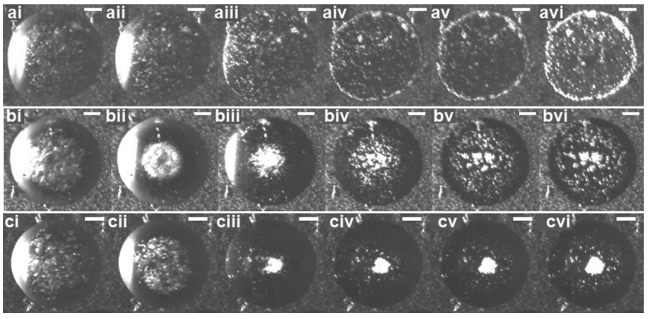

Figure 11. Drying droplets of 50 vol % ethanol containing 0.1 vol % of 755 nm polystyrene spheres and (a) 0.1 wt %, (b) 1 wt %, and (c) 3 wt % PSS (70 kg mol^{-1}) after (i) $0.1t_{dry}$, (ii) $0.2t_{dry}$, (iii) $0.5t_{dry}$, (iv) $0.8t_{dry}$, (v) $0.9t_{dry}$, and (vi) $1.0t_{dry}$. Scale bars are 20 μm. PSS concentrations are given in the water alone.

DOI: 10.1021/am5087177
ACS Appl. Mater. Interfaces 2015, 7, 3782−3790

without PSS. Particles were transported to the contact line during the radial flow period to form a ring stain (Figure 11avi). At 1 wt % PSS (i.e., 0.6 wt % in the entire suspension), some flocculation occurred in the collected group of particles, but the flocs were carried outward by convective flow in the latter stages of drying. The result was a deposit consisting of large particle flocs at the center and smaller particle flocs toward the contact line (Figure 11bvi). At a PSS concentration of 3 wt % (i.e., 1.7 wt % in the entire suspension), particle flocs "locked" together at the center of the droplet to form one large floc from which only a few single particles escaped via radial flow (Figure 11cvi). This large floc settled onto the substrate under gravity and remained at the center of the droplet, giving a deposit diameter of ~0.3R.

Figure 12 explores the effect of molecular weight on droplet drying. For higher molecular weights of PSS (300 and 500 kg mol^{-1}), lower concentrations of PSS are required to induce flocculation—which is desirable—but the viscosity also increases more quickly with molecular weight (Figure 13). If the viscosity increases too much during the early stages of drying, the Marangoni flows and the consequent particle migration are weaker (see Figure 12b,c). Figure 14 shows how the radius of the migrating group of particles varies with time for a range of concentrations of 300 kg mol^{-1} PSS. At PSS concentrations ≤0.5 wt %, the inward migration of particles was unhindered and the minimum radius of the collected group was the same as in the absence of PSS (~0.3R). When the PSS concentration increased to ≥1 wt %, the viscosity increase reduced migration, causing a wider collected group (~0.5R). As depletion flocculation is enhanced at higher particle concentrations,[27] the wider particle group makes depletion flocculation less efficient. We observed the formation of small aggregates that were transported toward the contact line by convection during the latter stages of drying with both 300 and 500 kg mol^{-1} PSS (Figure 12).

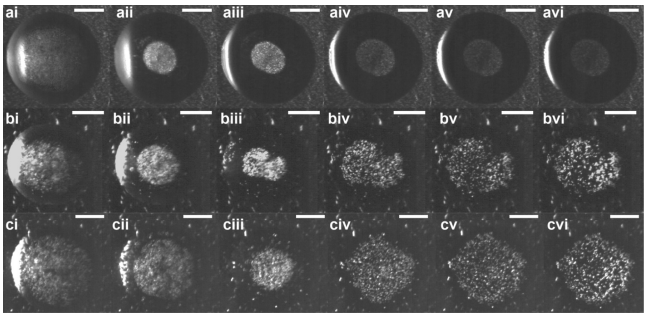

Figure 12. Drying droplets of 50 vol % ethanol containing 0.1 vol % of 755 nm polystyrene spheres and (a) 15 wt % PSS (35 kg mol^{-1}), (b) 0.3 wt % PSS (300 kg mol^{-1}), and (c) 0.3 wt % PSS (500 kg mol^{-1}) after (i) 0.1t_{dry}, (ii) 0.2t_{dry}, (iii) 0.5t_{dry}, (iv) 0.8t_{dry}, (v) 0.9t_{dry}, and (vi) 1.0t_{dry}. Scale bars are 50 μm. PSS concentrations are given in the water alone.

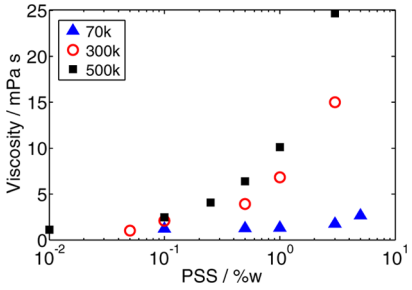

Figure 13. Dependence of the low-shear viscosity on the polymer concentration for various molecular weights of PSS.

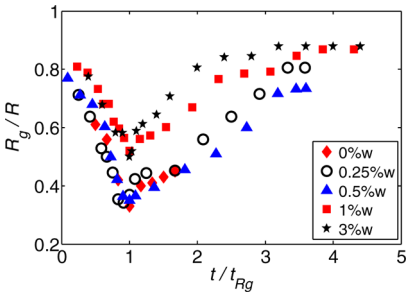

Figure 14. Evolution of the particle group radius, R_g, with time for a 50 vol % ethanol droplet containing 0.1 vol % of 755 nm spheres and various concentrations of PSS (300 kg mol^{-1}) in the water alone. R_g is normalized by the initial droplet contact radius, R, and the time is normalized by the time at which the group reaches a minimum radius, t_{R_g}.

For higher molecular weight samples, the depletion interaction acts over larger distances, forming flocs early on in the formation of a central particle group. There is also less mobility of particles within a floc, reducing rearrangement. These flocs do not form many contact points with other flocs in the group, so they do not create an interconnected structure. While the polymer concentration was high enough for flocculation (Table 2), the particle concentration was too low to form a single connected floc. The structure can then be pulled outward/apart by capillary flow (Figure 15a). In contrast, the lower molecular weight samples have a higher number of contact points, such that a single particle may have multiple weak depletion interactions, forming a strong interconnected particle floc overall. This large particle floc cannot be separated by capillary flow (Figure 15b).

For a lower molecular weight PSS (35 kg mol^{-1}) at concentrations up to 15 wt % in water, we observed particle migration to form a collected group of particles, but no aggregation. As the PSS concentration increased, particle motion toward the contact line was reduced in the latter stage of drying, probably due to a rapid increase in the viscosity of the solution as the solvent evaporates. The result was a circular deposit with good radial uniformity and a smaller diameter than the initial droplet (~0.4R; see Figure 12a). Increasing the PSS concentration further to 20 wt % to encourage depletion flocculation resulted in phase separation in the initial solution (50 vol % ethanol) due to the solubility limit of the PSS. The high polymer content in the 15 vol % suspension causes a large increase in viscosity throughout drying (particularly near the contact line), which could mean that it is not depletion flocculation that is retaining the central group but a polymer matrix. While the 15 wt % PSS solution in water does give a dot with a well-defined edge, there is a large amount of polymer deposited on the surface, which may be undesirable for applications (a small amount of polymer to act as a binder may be desirable).

Our experiments indicate an optimal polymer molecular weight around 70 kg mol^{-1} for generating a single dense floc of colloidal particles at the center of the evaporating droplet. Lower molecular weight polymers did not cause obvious depletion flocculation, and high concentrations were needed to inhibit radial convection, probably through the rapid increase in viscosity in the latter stages of drying. Higher molecular weight polymers tended to cause flocculation too early and led to a large number of small aggregates that migrated toward the contact line under convective flow. We also found an optimum polymer

DOI: 10.1021/am5087177
ACS Appl. Mater. Interfaces 2015, 7, 3782−3790

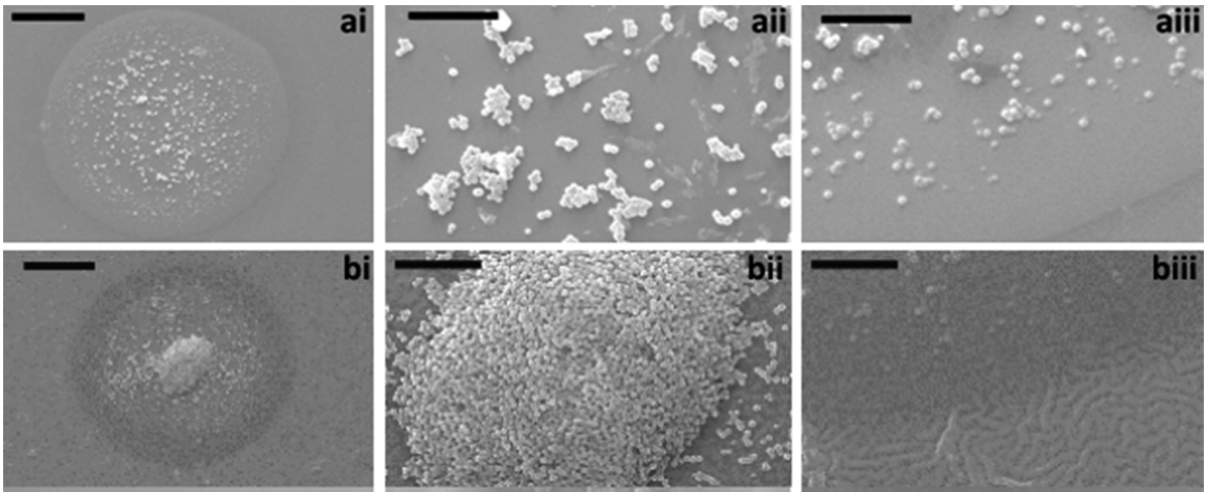

Figure 15. SEM images of deposits from dried 50 vol % ethanol/water droplets containing 0.1 vol % of 755 nm polystyrene spheres and (a) 0.5 wt % of 300 kg mol^{-1} PSS on glass or (b) 3 wt % of 70 kg mol^{-1} PSS on coated glass (hence the undulating features in part biii). Images show (i) the whole deposit and closeups of (ii) the deposit center and (iii) the contact line. Scale bars are 50 μm for the whole deposit and 10 μm for the closeups.

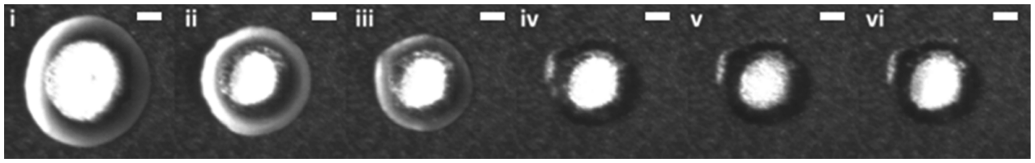

Figure 16. Sequence of images for a drying droplet containing 50 vol % ethanol/water, 3 wt % of 70 kg mol^{-1} PSS (in water alone), and 0.1 vol % of 775 nm polystyrene spheres on a coated glass substrate at (i) 0.1t_{dry}, (ii) 0.2t_{dry}, (iii) 0.5t_{dry}, (iv) 0.8t_{dry}, (v) 0.9t_{dry}, and (vi) 1.0t_{dry}. Scale bars are 20 μm.

concentration that induced aggregation at the point where the particles had formed the smallest central disk. Lower polymer concentrations did not prevent radial convection at the end of drying, while higher concentrations increased the viscosity and inhibited the inward migration of the particles under Marangoni flow. A higher polystyrene sphere concentration of 1 vol % also resulted in particle collection and a deposit comprising a single dot (Figure 16).

CONCLUSIONS

Drying picoliter droplets of ethanol/water exhibit Marangoni flows and particle migration, leading to the formation of a concentrated central group of particles during the Marangoni flow period. To prevent radial flow subsequently transporting particles to the contact line and forming a ring stain, two strategies were developed to maintain the central group in the deposit. The result was the printing of a small deposit from a large droplet, which may be of interest for security printing, since it generates a feature not readily reproduced by conventionally printed droplets. This method provides an alternative to current methods for printing small dots, which use retraction of the contact line to gather particles and require a smooth substrate. Unlike the proposed method, current methods are often hindered by the inclusion of particles that can cause the contact line to self-pin. The mechanism described in this paper also has potential for printing high-resolution lines for conductive screens. Alternative binary solvent mixtures can also be used to induce particle migration.

The first strategy used an evaporation-driven sol−gel transition to prevent particle motion in the gel through elasticity. Once the yield stress of the laponite suspension was sufficient to overcome the capillary flow, particle motion toward the contact line ceased. The recovery time of the network (following breakdown in the printhead) needed to be fast enough to form a gel shortly after the Marangoni flow period had ended, but not so fast that migration was inhibited. A lower ethanol concentration and higher laponite concentration proved to produce the best deposits. The minimum size achieved for the dry deposit was, however, significantly larger than the minimum size of the collected group of particles in the absence of laponite.

The second fixing strategy used polystyrenesulfonate (PSS) to induce depletion flocculation. A molecular weight of 70 kg mol^{-1} gave good interconnectivity between particle flocs at ∼2 wt % (in the entire solution), forming a dense, locked structure that was retained at the deposit center, forming a small dot. Under optimum conditions, the final deposit occupied an area less than 10% of that of the printed droplet. For higher molecular weights, less PSS was required for flocculation, but the particle flocs formed were loose and not interconnected. Consequently, capillary flow was able to pull the particle flocs apart and a wide group was formed as a deposit. There is enormous potential to tune the polymer/solvent/particle mixture to tailor formulations for a given application (i.e., the strategy is not limited to the use of PSS or polystyrene spheres).

ASSOCIATED CONTENT

Supporting Information

Additional videos of drying droplets containing laponite or PSS, corresponding to Figures 1, 8a, 11b,c, and Figure 12a. This material is available free of charge via the Internet at http://pubs.acs.org.

DOI: 10.1021/am5087177
ACS Appl. Mater. Interfaces 2015, 7, 3782−3790

AUTHOR INFORMATION

Corresponding Author

*E-mail: c.d.bain@durham.ac.uk.

Present Addresses

[¶]Briggs of Burton PLC, Briggs House, Derby St., Burton-on-Trent DE14 2LH, U.K.

[‖]Faculty of Engineering, Architecture and Information Technology, The University of Queensland, Brisbane, QLD 4072, Australia.

[⊥]Department of Mechanical Engineering, University of Wisconsin—Madison, Madison, WI 53706.

Notes

The authors declare no competing financial interest.

ACKNOWLEDGMENTS

The authors thank Dr. Olivier Cayre (University of Leeds) for his valued advice, and Dr. P. S. Brown and Prof. J. P. S. Badyal (Durham University) for the coated substrates. This work was supported financially by EPSRC under grant number EP/H018913/1.

REFERENCES

(1) Deegan, R. D.; Bakajin, O.; Dupont, T. F.; Huber, G.; Nagel, S. R.; Witten, T. A. Capillary Flow as the Cause of Ring Stains from Dried Liquid Drops. *Nature* **1997**, *389*, 827−829.

(2) Deegan, R. D.; Bakajin, O.; Dupont, T. F.; Huber, G.; Nagel, S. R.; Witten, T. A. Contact Line Deposits in an Evaporating Drop. *Phys. Rev. E* **2000**, *62*, 756−765.

(3) Hebner, T. R.; Wu, C. C.; Marcy, D.; Lu, M. H.; Sturm, J. C. Ink-Jet Printing of Doped Polymers for Organic Light Emitting Devices. *Appl. Phys. Lett.* **1998**, *72*, 519−521.

(4) Sirringhaus, H.; Kawase, T.; Friend, R. H.; Shimoda, T.; Inbasekaran, M.; Wu, W.; Woo, E. P. High-Resolution Inkjet Printing of All-Polymer Transistor Circuits. *Science* **2000**, *290*, 2123−2126.

(5) Yang, Y.; Chang, S.-C.; Bharathan, J.; Liu, J. Organic/Polymeric Electroluminescent Devices Processed by Hybrid Ink-Jet Printing. *J. Mater. Sci.: Mater. Electron.* **2000**, *11*, 89−96.

(6) Soltman, D.; Subramanian, V. Inkjet-Printed Line Morphologies and Temperature Control of the Coffee Ring Effect. *Langmuir* **2008**, *24*, 2224−2231.

(7) Fuller, S. B.; Wilhelm, E. J.; Jacobson, J. M. Ink-Jet Printed Nanoparticle Microelectromechanical Systems. *J. Microelectromech. Syst.* **2002**, *11*, 54−60.

(8) Molesa, S.; Redinger, D. R.; Huang, D. C.; Subramanian, V. High-Quality Inkjet-Printed Multilevel Interconnects and Inductive Components on Plastic for Ultra-Low-Cost RFID Applications. *Mater. Res. Soc. Symp. Proc.* **2003**, *769*, 253−258.

(9) Kim, D.; Moon, J. Highly Conductive Ink Jet Printed Films of Nanosilver Particles for Printed Electronics. *Electrochem. Solid-State Lett.* **2005**, *8*, J30−J33.

(10) Lee, D. J.; Oh, J. H. Shapes and Morphologies of Inkjet-Printed Nanosilver Dots on Glass Substrates. *Surf. Interface Anal.* **2010**, *42*, 1261−1265.

(11) Okamoto, T.; Suzuki, T.; Yamamoto, N. Microarray Fabrication with Covalent Attachment of DNA using Bubble Jet Technology. *Nat. Biotechnol.* **2000**, *18*, 438−441.

(12) Roth, E. A.; Xu, T.; Das, M.; Gregory, C.; Hickman, J. J.; Boland, T. Inkjet Printing for High-Throughput Cell Patterning. *Biomaterials* **2004**, *25*, 3707−3715.

(13) Hu, H.; Larson, R. G. Marangoni Effect Reverses Coffee-Ring Depositions. *J. Phys. Chem. B* **2006**, *110*, 7090−7094.

(14) Park, J.; Moon, J. Control of Colloidal Particle Deposit Patterns within Picoliter Droplets Ejected by Ink-Jet Printing. *Langmuir* **2006**, *22*, 3506−3513.

(15) Lim, J. A.; Lee, W. H.; Lee, H. S.; Lee, J. H.; Park, Y. D.; Cho, K. Self-Organization of Ink-Jet-Printed Triisopropylsilylethynyl Pentacene via Evaporation-Induced Flows in a Drying Droplet. *Adv. Funct. Mater.* **2008**, *18*, 229−234.

(16) Kajiya, T.; Kobayashi, W.; Okuzono, T.; Doi, M. Controlling the Drying and Film Formation Processes of Polymer Solution Droplets with Addition of Small Amount of Surfactants. *J. Phys. Chem. B* **2009**, *113*, 15460−15466.

(17) Still, T.; Yunker, P. J.; Yodh, A. G. Surfactant-Induced Marangoni Eddies Alter the Coffee-Rings of Evaporating Colloidal Drops. *Langmuir* **2012**, *28*, 4984−4988.

(18) Hu, H.; Larson, R. G. Analysis of the Effects of Marangoni Stresses on the Microflow in an Evaporating Sessile Droplet. *Langmuir* **2005**, *21*, 3963−3971.

(19) Hamamoto, Y.; Christy, J. R. E.; Sefiane, K. The Flow Characteristics of an Evaporating Ethanol Water Mixture Droplet on a Glass Substrate. *J. Therm. Sci. Technol.* **2012**, *7*, 425−436.

(20) Talbot, E. L.; Berson, A.; Bain, C. D. Drying and Deposition of Picolitre Droplets of Colloidal Suspensions in Binary Solvent Mixtures. *NIP28: 28th International Conference on Digital Printing Technologies. Digital Fabrication 2012. September 2012*; Society for Imaging Science and Technology: Springfield, VA, 2012; Vol. *28*, pp 420−423, ISBN 978-89208-302-2.

(21) Talbot, E. L.; Berson, A.; Yang, L.; Bain, C. D. Internal Flows and Particle Transport Inside Picoliter Droplets of Binary Solvent Mixtures. *NIP29: 29th International Conference on Digital Printing Technologies. Digital Fabrication 2013. September/October 2013*; Society for Imaging Science and Technology: Springfield, VA, 2013; Vol. *29*, pp 307−312, ISBN 978-89208-306-0.

(22) Talbot, E. L.; Yang, L.; Berson, A.; Bain, C. D. Control of Particle Distribution in Inkjet Printing Through an Evaporation-Driven Sol−Gel Transition. *ACS Appl. Mater. Interfaces* **2014**, *6*, 9572−9583.

(23) Mourchid, A.; Delville, A.; Levitz, P. Sol−Gel Transition of Colloidal Suspensions of Anisotropic Particles of Laponite. *Faraday Discuss.* **1995**, *101*, 275−285.

(24) Seebergh, J. E.; Berg, J. C. Depletion Flocculation of Aqueous, Electrosterically-Stabilized Latex Dispersions. *Langmuir* **1994**, *10*, 454−463.

(25) Sharma, A.; Tan, S. N.; Walz, Y. Effect of Nonadsorbing Polyelectrolytes on Colloidal Interactions in Aqueous Mixtures. *J. Colloid Interface Sci.* **1997**, *191*, 236−246.

(26) Sharma, A.; Tan, S. N.; Walz, Y. Measurement of Colloidal Stability in Solutions of Simple, Nonadsorbing Polyelectrolytes. *J. Colloid Interface Sci.* **1997**, *190*, 392−407.

(27) Burns, J. L.; Yan, Y.; Jameson, G. J.; Biggs, S. The Effect of Molecular Weight of Nonadsorbing Polymer on the Structure of Depletion-Induced Flocs. *J. Colloid Interface Sci.* **2002**, *247*, 24−32.

(28) Woodward, I.; Schofield, W. C. E.; Roucoules, V.; Badyal, J. P. S. Super-Hydrophobic Surfaces Produced by Plasma Fluorination of Polybutadiene Films. *Langmuir* **2003**, *19*, 3432−3438.

(29) Yow, H. N.; Biggs, S. Probing the Stability of Sterically Stabilized Polystyrene Particles by Centrifugal Sedimentation. *Soft Matter* **2013**, *9*, 10031−10041.

(30) Herrera, N. N.; Letoffe, J.-M.; Putaux, J.-L. Aqueous Dispersions of Silane-Functionalized Laponite Clay Platelets: A First Step toward the Elaboration of Water-Based Polymer/Clay Nanocomposites. *Langmuir* **2004**, *20*, 1564−1571.

DOI: 10.1021/am5087177
ACS Appl. Mater. Interfaces 2015, 7, 3782−3790